Analytic model for transient anomalous diffusion with highly persistent correlations

Sean Carnaffan[*] and Reiichiro Kawai[†]

School of Mathematics and Statistics, University of Sydney, NSW 2006, Australia

In recent decades, many stochastic processes have been proposed as models for real world time series data with anomalous spreading, highly persistent correlations, and transient distributional characteristics. We introduce the higher order fractional tempered stable motion as the stochastic integral of the tempered stable motion with respect to a generalized higher order moving average kernel, which provides an analytic model for stochastic processes possessing these characteristics. This stochastic process provides a mathematical model for anomalous diffusion with a transient distribution resembling higher order fractional stable motion on short timescales and higher order fractional Brownian motion in the long run. The specifics of the crossover dynamics from the Lévy stable anomalous diffusion to the Gaussian anomalous diffusion are controlled by explicit parameter values that correspond to physical attributes of the process. It is well suited to modeling anomalous diffusion of any "type" (sub-, super-, regular, or hyperdiffusion) under appropriate parametrizations due to its power-law scaling of variance with respect to time. It is also a useful model for position-velocity-acceleration triples due to its convenient path differentiability and integrability properties. To highlight the potential physical relevance of this model for real world data, we outline its key statistical properties including its covariance structure, memory, and second order self-similarity. We also give an easy to implement elementary method for sample path generation which may be used as a basis for simulation and Monte Carlo studies.

I. INTRODUCTION

Observations of diffusions which deviate from "normal" or "regular" diffusion have become ubiquitous in the literature of statistical physics, marking a paradigm shift from the classical diffusion of Fick and Einstein to the so-called "anomalous" diffusion. Anomalous diffusions are typically identified through the ensemble mean squared displacement. In contrast to the proportionality of variance with respect to time observed in Brownian motion, anomalous diffusions exhibit a nonlinearity, particularly a power-law dependency. Such behavior has been observed in soft matter and plasma physics via the diffusion of hydrogen in metals and the movement of holes in semiconductor alloys [1–4], in organic chemistry and biology via anomalous protein diffusion in cells due to crowding [5–7], and in astrophysics and cosmology via the motion of bright spots on the Sun and the subdiffusion of cosmic rays [8–11]. These types of motion often emerge as a result of correlations in trajectories which either exacerbate or inhibit the spread of test particles depending on whether it is a positive or a negative correlation. This type of motion is therefore often described by the fractional Brownian motion (fBm), in which a Brownian motion serves as a stochastic integrator with respect to a moving average kernel [12]. However, the usual fBm has been shown to be insufficient to model some time series data with highly persistent correlations apparent in their power spectra. In particular, when analyzing the spectrum of some time series data, such as Nile river data [13] and

bone radiograph data [14], for example, the Hurst parameter exceeds one. Therefore, higher order models of the fBm were introduced to capture these more persistent correlations [15] This was done by generalizing the moving average integration kernel in the construction of the fBm. This stochastic process was called higher order fractional Brownian motion (n-fBm).

Concurrently, a range of motions observed in nature have been characterized by the emergence of non-Gaussian (particularly heavy-tailed) marginal probability distributions. As a result, Lévy-flight behavior and Lévy distributions have been in vogue topics of study in recent decades [16]. In particular, these stochastic descriptions arise in the modeling of test particles that occasionally undergo long-range jumps. This type of motion is routinely observed in diverse fields such as share market data in finance [17–19], flows and turbulence in fluid mechanics [20,21], and mathematical ecology [22–24]. In the latter, the hypothesized optimality of this form of motion for search procedures is known as the Lévy flight optimal foraging hypothesis [25]. The essential features of the Lévy flight model are the divergence of the second moment of the distribution of jump sizes and the subsequent scale invariance of this distribution. However, the observations of transient and regime changing distributional behavior for stochastic processes has motivated the study of tempered stable distributions, whose tempering of these larger jumps force stable law type behavior on short time scales and Gaussian behavior in the long run. Such stochastic models have found success in modeling many physical phenomena as well as resolving the apparent physical absurdity of heavy-tailed jump distributions which imply that physical objects may jump arbitrarily large distances with nonvanishing probability [26–31].

─────────
[*]Corresponding author: seanc@maths.usyd.edu.au
[†]reiichiro.kawai@sydney.edu.au

Combining the ideas of Lévy flight type motion and higher order correlated motion, the higher order fractional stable motion was introduced in [32]. This adapted the definition of the higher order fBm [15] to the case where the driving noise (the stochastic integrator) was a symmetric stable Lévy process. This was called nth order fractional stable motion (n-fsm) and was demonstrated to be a model for heavy-tailed hyperdiffusion (with an admitted slight abuse of terminology in that the variance of the n-fsm is infinite). To provide the next step in terms of generalizing these models, in the present work we consider the case where the driving noise serving as the integrator for a higher order moving average kernel is the tempered stable motion. This allows us to introduce a process, which we call higher order fractional tempered stable motion (n-ftsm), which has higher order correlations in its sample paths, but has the technical advantage of having a finite second moment and therefore a well defined covariance structure. Moreover, the model we introduce has a transient distribution in that in the short time limit it resembles the n-fsm [32], and in the long run exhibiting aggregate Gaussianity, particularly a convergence to the higher order fBm [15]. The respective rates of convergence to these stochastic processes are controlled by the (generalized) Hurst parameter and may therefore be controlled to suit the specific data acquired from an experiment. The n-ftsm also has the capacity to model sub-, regular, super-, ballistic, and hyperdiffusion depending on parameter choice. The model also carries the convenient analytical property of path differentiability, and particularly the result that the derivative of an n-ftsm is an $(n-1)$-ftsm. This suggests that the n-ftsm may be useful in modeling the position, velocity, and acceleration triplets of individual test particles via successive integration or differentiation.

We provide an analysis of the properties of n-ftsm as well as a simulation scheme. We illustrate typical trajectories of the n-ftsm and demonstrate its short run convergence to n-fsm [32] and long run convergence to n-fBm [15] empirically and theoretically. We also demonstrate how parameter estimation may be performed in practice via a simulation study.

The n-ftsm provides a model for motion which is qualitatively similar to the n-fsm, but due to the finite moments of the driving tempered stable motion has a similar level of analytical tractability as the n-fBm. In particular, in contrast to the n-fsm [32], the existence of second order properties allows us to consider covariance structure and memory. Moreover, the long run Gaussianity of the n-ftsm suggests it may be a useful modeling tool for transient anomalous diffusion processes in nature [33–36].

Throughout the text, we present the most pertinent details of each section at the beginning and send much of the technical detail to the Appendixes to maintain the flow of the paper.

II. MODEL

Consider a càdlàg version of the tempered stable motion $\{L_t^{\alpha,\beta}\}_{t\in\mathbb{R}}$, that is, the two sided pure jump process governed by the symmetric Lévy measure

$$\nu(dz) = \frac{\alpha c_\alpha}{2} \frac{e^{-\beta|z|}}{|z|^{\alpha+1}} dz, \qquad (2.1)$$

for $z \in \mathbb{R}\backslash\{0\}$, where $\alpha \in (0,2)$, $c_\alpha = [\cos(\pi\alpha/2)\Gamma(1-\alpha)]^{-1}$, and $\beta > 0$. The tempered stable motion (which has found application in modeling telecommunication networks, daily hydrological series, and turbulence; see for example [35,37]) is a Lévy process whose Lévy measure is exponentially suppressed in the tail (relative to that of a stable process) inducing finite polynomial moments of all orders. This means that on short time scales small jumps dominate the trajectory, allowing the process to resemble stable motion, but forcing the process to adhere to central limit theorem type dynamics in the long run. The constant c_α in the Lévy measure (2.1) is continuous in α and is introduced into the Lévy measure to simplify constants in the simulation scheme which we will give in Sec. VI. The Lévy measure (2.1) implies that the unit time marginal $L_1^{\alpha,\beta}$ admits the characteristic exponent

$$\phi_{\alpha,\beta}(y) := \ln\mathbb{E}\big[e^{iyL_1^{\alpha,\beta}}\big] = \int_{\mathbb{R}\backslash\{0\}} (e^{iyz} - 1 - iyz)\nu(dz)$$

$$= \frac{\alpha c_\alpha \beta^\alpha \Gamma(-\alpha)}{2}\left[\left(1 + \frac{iy}{\beta}\right)^\alpha + \left(1 - \frac{iy}{\beta}\right)^\alpha - 2\right], \qquad (2.2)$$

for $y \in \mathbb{R}$ where ν is as in definition (2.1). With the above definition of tempered stable motion in place, we may define the n-ftsm as follows.

Definition 2.1. Let $\alpha \in (0,2)$, $\beta > 0$, $n \in \mathbb{N}$, and $H > 0$ such that $H - 1/\alpha \in (n - 3/2, n - 1/2)$. We define the nth-order fractional tempered stable motion $\{L_{H,\alpha,\beta}^n(t)\}_{t\geqslant 0}$ as

$$L_{H,\alpha,\beta}^n(t) := \int_{\mathbb{R}} f_n(t,s;H,\alpha)dL_s^{\alpha,\beta}, \quad t \geqslant 0,$$

where the integrand is the higher order moving average kernel

$$f_n(t,s;H,\alpha) := \frac{1}{\Gamma(H+1-1/\alpha)}\left[(t-s)_+^{H-1/\alpha}\right.$$

$$\left. - \sum_{k=0}^{n-1}\binom{H-1/\alpha}{k}t^k(-s)_+^{H-1/\alpha-k}\right],$$

for $s \in \mathbb{R}$ and $t \geqslant 0$.

In the above definition and throughout, $\binom{n}{k} := n(n-1)\cdots(n-k+1)/k!$; values of the gamma function for negative inputs are determined by the usual analytic continuation. For $a \in \mathbb{R}$, the notation $(a)_+$ denotes the maximum of a and zero. Due to the zero-power convention $0^0 := 1$, we have $f_n(0,s;H,\alpha) = 0$ for all $s \in \mathbb{R}$, which implies $L_{H,\alpha,\beta}^n(0) = 0$ almost surely.

The higher order motion in Definition II.1 is a generalization of tempered stable and first order fractional tempered stable motions as it includes these processes as base cases. In particular, in the case where $n = 1$, the moving average kernel $f_1(t,s;H,\alpha)$ becomes the usual moving average kernel $[(t-s)_+^{H-1/\alpha} - (-s)_+^{H-1/\alpha}]/\Gamma(H+1-1/\alpha)$ and therefore the resultant integrated process is a (first-order) fractional tempered stable motion, in analogous sense to the fBm. In particular, the kernel $f_n(t,s;H,\alpha)$, analogous to the integration kernel of the n-fBm [15], is constructed by subtracting from the usual first order moving average kernel $(t-s)_+^{H-1/\alpha}$ the first $n-1$ terms of its Taylor expansion in s around zero.

Also, in the case where $H = 1/\alpha$, we recover simply the underlying tempered stable motion as $f_n(t, s; 1/\alpha, \alpha) = \mathbb{1}(s \in [0, t))$ using the aforementioned zero-power convention. A first order fractional tempered stable motion with a Volterra kernel with compact support is investigated in [38].

Due to the characteristic function of stochastic integrals [39], we have $\ln \mathbb{E}[e^{iyL_{H,\alpha,\beta}^{n(t)}}] = \int_{\mathbb{R}} \phi_{\alpha,\beta}(y f_n(t, s; H, \alpha)) ds$ as the characteristic exponent of the n-ftsm. The evenness of the charasteristic function $\phi_{\alpha,\beta}$ of the driving noise from (2.2) then ensures that the characteristic function of the n-ftsm is even, and therefore the n-ftsm has a symmetrical distribution at all times—an observation which is not obvious from the definition (II.1) due to the asymmetry of the integration kernel. Specifically, the n-ftsm has zero mean at all times for all $n \geqslant 1$.

III. SAMPLE PATH PROPERTIES

From a mathematical perspective, it is prudent to verify that the sample map $t \to L_{H,\alpha,\beta}^n(t)$ is almost surely well defined. We therefore first consider the existence of the n-ftsm in the sense of trajectories not diverging to infinity, that is, parameter settings under which, for each fixed $T > 0$, trajectories of the n-ftsm do not explode in the sense $\mathbb{P}(\sup_{t\in[0,T]} |L_{H,\alpha,\beta}^n(t)| = \infty) = 1$, rendering the n-ftsm of little practical interest [38,40]. The sample paths of the fractional tempered stable motion are almost surely unbounded on every interval of finite length whenever $\alpha \in [0, \min(2, 1/(n-1))]$ and $H \in [n-1, \min(n, 1/\alpha)]$ [32,38]. For the remainder of this paper, we therefore assume that we are outside this parameter setting. This restriction does not exclude too many instances of the n-ftsm since, for instance, choosing $\alpha > 1/(n-1)$ will automatically avoid this sample unboundedness regardless of the choice of H, and this range of values for α increases as n increases.

The integral (2.1) is well defined as a stochastic integral in the Itô sense as the integrator $\{L_t^{\alpha,\beta}\}_{t\geqslant 0}$ is a Lévy process and therefore a semimartingale. We note also the integral and differential recurrence relations of the kernel: $\int_0^t f_n(v, s; H, \alpha) dv = f_{n+1}(t, s; H + 1, \alpha)$ and $\frac{\partial}{\partial t} f_n(t, s; H, \alpha) = f_{n-1}(t, s; H - 1, \alpha)$, where the latter (differential) relation holds for $n \geqslant 2$. As a result, one may show the integral relation

$$\left\{ L_{H,\alpha,\beta}^n(t) \right\}_{t\geqslant 0} \stackrel{\mathscr{L}}{=} \left\{ \int_0^t L_{H-1,\alpha,\beta}^{n-1}(s) ds \right\}_{t\geqslant 0}, \quad (3.1)$$

relating orders of the n-ftsm for $n \geqslant 2$ and $\alpha \in [1, 2)$. Moreover, sample paths of the n-ftsm are differentiable, with

$$\left\{ \frac{\partial}{\partial t} L_{H,\alpha,\beta}^n(t) \right\}_{t\geqslant 0} \stackrel{\mathscr{L}}{=} \left\{ L_{H-1,\alpha,\beta}^{n-1}(t) \right\}_{t\geqslant 0},$$

for $n \geqslant 2$ and $\alpha \in [1, 2)$. This shows that if, for example, the location of a particle is well modeled by the n-ftsm, then its associated velocity process follows an $(n-1)$-ftsm model (and vice versa). Therefore, the family of higher order fractional tempered stable motions introduced here models location-velocity-acceleration triplets, since the position process may be differentiated (and differentiated again) to yield the corresponding velocity process (and acceleration process)
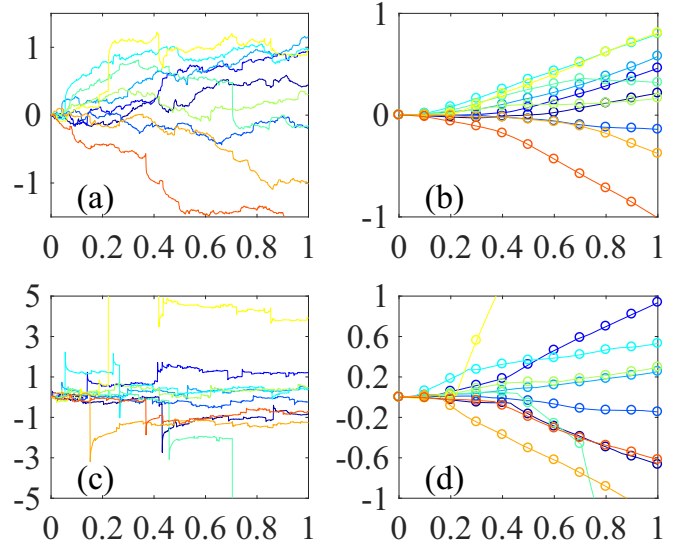

FIG. 1. Typical trajectories of n-ftsm. Parameters used were (top row) $\alpha = 1.5$, $\beta = 1$, and $H = n - 0.2$ and (bottom row) $\alpha = 1.1$, $\beta = 0.1$, and $H = n - 0.2$. In both rows we put (a) and (c) trajectories of 1-ftsm generated using (6.1) and (b) and (d) trajectories of 2-ftsm produced using successive cumulative integration of the 1-ftsm in (a) as per integral relation (3.1) (circles) as well as using (6.1) with the same background noise (common sequence of jumps) as in the $n = 1$ case. In the top row, the larger values of α and β stifle large jumps in the driving noise making the motion appear continuous, while in the bottom row the relatively smaller values of α and β ensure the presence of occasional large jumps in the background noise, leading to occasional jumplike displacements in the integrated motion. However, since the parameter setting used in (c) (in particular, $2G = 0.7818 < 1$) gives antipersistent behavior (subdiffusive spread and short memory) the sample path tends to revert back to its mean after each displacement.

in a manner that is not only well defined but ensures the resulting processes are still in the higher order fractional tempered stable family of motions. Typical sample trajectories are illustrated in Fig. 1.

IV. SECOND ORDER PROPERTIES

Since this model is being proposed under the class of anomlous diffusion models, it is natural to consider the variance of the process. However, much physical insight about population behaviors of the n-ftsm may be gained by looking at other more general second order moment properties. Therefore, we consider the autocovariance structure which tells us about the variance scaling with time, second order self-similarity, and memory. These second order properties, which all have to do with spreading and persistence of correlations, are the ones that demonstrate when the n-ftsm would be most relevant as a physical model, as well as provide a potential theoretical basis for model selection and parameter inference in future empirical study using the n-ftsm.

Thanks to the tempered stable integrator $\{L_t^{\alpha,\beta}\}_{t\in\mathbb{R}}$ being centered and possessing finite mean (as opposed to the case of n-fsm [32]), the covariance structure of the higher order fractional tempered stable motion exists and may be calculated

using the Wiener-Itô isometry. Separately, we point out that, due to the nonuniqueness of the kernel with respect to the parameters H and $1/\alpha$, we have the identity $f_n(t, s; H, \alpha) = f_n(t, s; H - 1/\alpha + 1/2, 2)$ and therefore, defining $G := H - 1/\alpha + 1/2$, our kernel exactly coincides with the kernel for the higher order fractional Brownian (n-fBm) of [15] with H replaced by G, from which many key second order and distributional results follow. The parameter G may then be seen in a sense to generalize the Hurst parameter H for fBm, to the case where the driving noise has a stability parameter not equal to two, as in the Gaussian case. However, the fact that the H must be replaced by a different parameter, G, in order for second moment and long run distributional properties to hold has the effect of essentially "breaking" the self-similarity in distribution of both the higher order fractional Brownian motion [15] and the higher order stable motion [32] as the n-ftsm is no longer self-similar in law.

Recalling $G = H - 1/\alpha + 1/2 \in (n - 1, n)$ due to Definition II.1, we have the following expression for the covariance structure of the process $\{L^n_{H,\alpha,\beta}(t)\}_{t \geqslant 0}$ for $0 \leqslant s \leqslant t$,

$$
\begin{aligned}
&\mathrm{Cov}\big(L^n_{H,\alpha,\beta}(s), L^n_{H,\alpha,\beta}(t)\big) \\
&= \gamma^2_{\alpha,\beta} C^n_G \Bigg[(t - s)^{2G} - \sum_{j=0}^{n-1} (-1)^j \binom{2G}{j} \left(\left(\frac{t}{s}\right)^j s^{2G} \right. \\
&\quad \left. + \left(\frac{s}{t}\right)^j t^{2G} \right) \Bigg],
\end{aligned}
$$
(4.1)

where $C^n_G := 1/(\Gamma(2G + 1)|\sin(\pi G)|)$ and $\gamma^2_{\alpha,\beta} := \beta^{\alpha-2}\alpha(1 - \alpha)/\cos(\pi\alpha/2)$ is the variance of the unit time marginal of the tempered stable motion for $\alpha \neq 1$ (see Appendix A for a derivation of this result). We point out that the superscript "n" in the symbol C^n_G does not refer to an nth power but is rather an index emerging from the recursion formula (A4), while the superscript "2" in $\gamma^2_{\alpha,\beta}$ does denote a square. The covariance (4.1) implies the power law scaling of variance

$$
\mathrm{Var}\big(L^n_{H,\alpha,\beta}(t)\big) = 2\gamma^2_{\alpha,\beta} C^n_G \binom{2G - 1}{n - 1} t^{2G},
$$
(4.2)

since $\sum_{j=0}^{n-1}(-1)^j\binom{2G}{j} = (-1)^{n-1}\binom{2G-1}{n-1}$. This is in analogy to the higher order fBm and demonstrates that in the mean squared displacement sense, the higher order fractional tempered stable motion can model sub-, super-, or hyperdiffusion depending on the value of the exponent $2G$ which can freely be varied by increasing the order n. In particular, higher order motions induce more hyperdiffusive spread. Furthermore, this variance scaling proves that the n-ftsm has nonstationary increments and is therefore nonergodic. Finally, the variance (4.2) immediately implies self-similarity of the second order moments of the process. That is,

$$
\mathrm{Var}\big(L^n_{H,\alpha,\beta}(ct)\big) = c^{2G}\mathrm{Var}\big(L^n_{H,\alpha,\beta}(t)\big),
$$

for any positive constant c. We note, though, that this self-similarity does not extend to the law of n-ftsm as it does for stable motions and the n-fBm. In the latter case, Gaussianity and second order self-similarity are sufficient to enforce self-similarity in law. We note that although the loss of self-similarity in law entails the loss of some useful analytical properties and fracticality, this is a necessary loss for the gain of a transient distribution. Furthermore, the n-ftsm is asymptotically self-similar fractal in both its short- and long-run regimes and is therefore approximately fractal.

The availability of the covariance structure in closed form means we may examine the short and long range memory properties of the process. These properties describe the long term persistence of correlation of increments. The concept of memory for stochastic processes is widely examined in econometrics and econophysics, particularly when the driving processes are Lévy noises [41–43]. To examine this correlation structure, we first introduce the differencing operator at lag $h > 0$, $\Delta_h X(t) := X(t + h) - X(t)$. For the higher order fractional tempered stable motion, we have due to (4.1) the asymptotics as $t \to \infty$ holding h constant,

$$
\mathrm{Cov}\big(\Delta_h L^n_{H,\alpha,\beta}(0), \Delta_h L^n_{H,\alpha,\beta}(t)\big) \sim 2(G - 1)\gamma^2_{\alpha,\beta} C^n_G h^2 t^{2(G-1)}.
$$
(4.3)

From this we may see that the n-ftsm has long memory, in the sense that, for each $h > 0$, the sum

$$
\sum_{k=0}^{\infty} \big| \mathrm{Cov}\big(\Delta_h L^n_{H,\alpha,\beta}(0), \Delta_h L^n_{H,\alpha,\beta}(kh)\big) \big|
$$

diverges whenever $2(G - 1) > -1$, that is, whenever $G > 1/2$, which is equivalent to $H > 1/\alpha$. We remark that, since $G \in (n - 1, n)$, this implies that short memory is only consistent with the parameter setting $n = 1$ with $H < 1/\alpha$; all higher order motions exhibit long memory. Indeed, this covariance term is not even decaying for sufficiently large G, despite the fact that the two increments being correlated are separating in time. To enforce the correlation of these departing increments to decay to zero, it is necessary to look at higher order (specifically nth order) differencing as in [15,32]. To these ends, we recursively define the nth order differencing operator at lag $h > 0$ by $\Delta^n_h X_t := \Delta^{n-1}_h X_{t+h} - \Delta^{n-1}_h X_t$ for integer $n > 1$, where the base Δ_h is the usual first order differencing operator. The covariance of the nth-order differenced n-ftsm at lag kh for positive integer k is then given by

$$
\begin{aligned}
&\mathrm{Cov}\big(\Delta^n_h L^n_{H,\alpha,\beta}(t), \Delta^n_h L^n_{H,\alpha,\beta}(t + kh)\big) \\
&= \gamma^2_{\alpha,\beta} C^n_G (-1)^n \sum_{j=-n}^{n} (-1)^j \binom{2n}{n + j} |(k + j)h|^{2G}.
\end{aligned}
$$
(4.4)

The resulting noise process is therefore weakly stationary since this covariance depends only on the lag kh and not on t, a fact which we exploit in the numerical experiment in Sec. VI regarding parameter fitting. The resulting stationary time series after n-times differencing has been referred to as fractional gray noise in [15]. The autocorrelation function at lag kh is given by, normalizing by the variance,

$$
\begin{aligned}
&\mathrm{Corr}\big(\Delta^n_h L^n_{H,\alpha,\beta}(t), \Delta^n_h L^n_{H,\alpha,\beta}(t + kh)\big) \\
&= \frac{\sum_{j=-n}^{n}(-1)^j\binom{2n}{n+j}|(k + j)h|^{2G}}{\sum_{j=-n}^{n}(-1)^j\binom{2n}{n+j}|jh|^{2G}},
\end{aligned}
$$
(4.5)

which we note is independent of α and β due to self-normalization. Finally we note that the autocovariance (4.4) leads to the asymptotics as $k \to \infty$

$$\left|\text{Cov}\left(\Delta_h^n L_{H,\alpha,\beta}^n(0), \Delta_h^n L_{H,\alpha,\beta}^n(kh)\right)\right| \sim D_{G,\alpha,\beta} h^{2G} k^{2G-2n},$$

where $D_{G,\alpha,\beta} := C_G \gamma_{\alpha,\beta}^2 (2G)(2G-1) \cdots (2G-2n+2)(2G-2n)$. Therefore, the correlation of the nth order difference n-ftsm decays to zero as a power law yielding short memory whenever $n > G + 1/2$ and long memory otherwise.

The divergence of the correlation of two departing increments (4.3) justifies the claim that the n-ftsm is "highly" correlated and is a remnant of the fact that higher order motions are produced via successive integration of lower order motions, increasing the correlation with each integral. We therefore hypothesize that the most physically relevant applications of the n-ftsm for particle motion may lie in the case where $n = 2$ such that the velocity process (which would be a 1-ftsm) is correlated but may have long or short memory depending on the physics of the scenario (or similarly $n = 3$ where the associated "acceleration process" exhibits this property) but the position process necessarily has long memory (to the point of increase of correlation in time).

V. SHORT AND LONG RUN DISTRIBUTIONS

A key property of the n-ftsm is its transient distribution. In the short run it behaves like a Lévy flight type process and in the long run behaves like a Gaussian process. Stochastic processes with transient distributions, particularly those combining stable and Gaussian trends, are ubiquitous in many domains of the natural sciences, such as turbulence modeling [44], hydrological modeling [45], and wind speed modeling [31]. This property therefore demonstrates the potential usefulness of the n-ftsm to model some of the many transient processes in nature, provided they possess highly persistent correlations. Specifically, we have the following convergences:

$$\left\{h^{-H} L_{H,\alpha,\beta}^n(ht)\right\}_{t\geqslant 0} \xrightarrow{\mathscr{L}} \left\{L_{H,\alpha}^n(t)\right\}_{t\geqslant 0}, \quad (5.1)$$

$$\left\{h^{-G} L_{H,\alpha,\beta}^n(ht)\right\}_{t\geqslant 0} \xrightarrow{\mathscr{L}} \left\{\gamma_{\alpha,\beta} B_G^n(t)\right\}_{t\geqslant 0}, \quad (5.2)$$

where $\{L_{H,\alpha}^n(t)\}_{t\geqslant 0}$ is a higher order fractional stable motion as in [32] is the n-fsm and $\{B_G^n(t)\}_{t\geqslant 0}$ is the n-fBm [15] with generalized Hurst parameter $G(=H - 1/\alpha + 1/2)$. The short run convergence (5.1) holds as $h \to 0$ and the long run convergence (5.2) as $h \to \infty$. Moreover, the convergence rates are controlled respectively by the Hurst parameter H and the generalized Hurst parameter G, meaning that the specifics of the crossover dynamics between the stable and Gaussian regimes may be controlled to suit experimental data. These convergences should be understood as convergence of all finite dimensional distributions, which follows in a similar manner as [28,38]. An elementary sketch of convergence in distribution is provided in the Appendixes for the purpose of providing intuition.

For a given $t > 0$, the random variable $L_{H,\alpha}^n(t)$ on the right hand side of (5.1) has a symmetric stable distribution whose parameters are given in [32] and the random variable $\gamma_{\alpha,\beta} B_G^n(t)$ has a Gaussian distribution with zero mean and
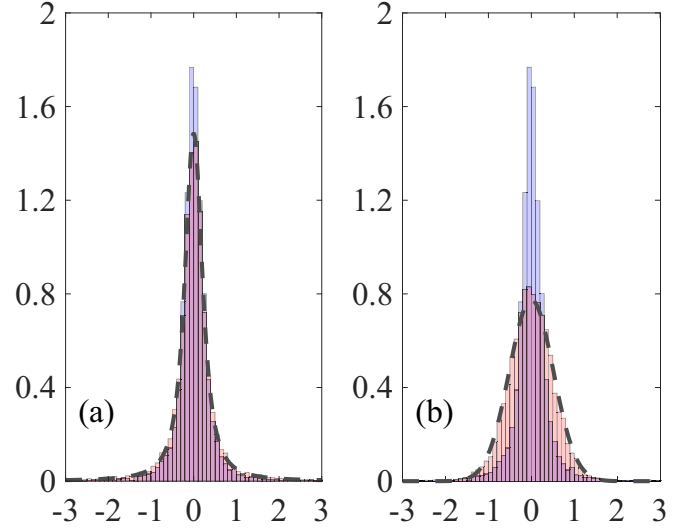

FIG. 2. Short and long run convergence of n-ftsm: histograms of 10^4 simulated trajectories with corresponding densities of limiting process. Parameters used were $n = 3$, $\alpha = 1.2$, $\beta = 0.1$, $H = 2.8$, $\kappa = 50$, and $m = 5000$ (see Sec. VI for details on these parameters). (a) Short run convergence demonstrated by simulating the left hand side of (5.1) with $h = 0.001$ (foreground, darker). (b) Long run convergence demonstrated by simulating the left hand side of (5.2) with $h = 1000$ (foreground, darker). In both figures, the lighter background histogram is of the $h = 1$ case given by (6.1) and the dotted red lines are the density functions of the respective theoretical limiting distributions given in Sec. V. Good agreement between the empirical histograms and theoretical limiting density functions is seen.

variance equal to that of the n-ftsm, $\text{Var}(L_{H,\alpha,\beta}^n(t))$, which is given by (4.2). We demonstrate the agreement between these short- and long-run limiting distributions and histograms of simulations of the n-ftsm in Fig. 2.

VI. SIMULATION METHOD

Infinite series representations of Lévy jump processes, such as those of [46] and others, are an extremely useful and tractable tool for designing simulation schemes for Lévy driven stochastic integrals. In particular, simulations of the n-ftsm on the compact interval $[0, T]$ for some fixed $T > 0$ may be performed by simulating an approximating process $\{L_{H,\alpha}^n(t; \kappa, m)\}_{t\in[0,T]}$, where κ and m are truncation parameters (more details in the Appendixes) affecting the error in the approximation (convergence in finite dimensional law occurs as $\kappa, m \to \infty$) defined as

$$\left\{L_{H,\alpha,\beta}^n(t; \kappa, m)\right\}_{t\in[0,T]}$$

$$\overset{\mathscr{L}}{=} \left\{\sum_{k=1}^{Z_{\kappa,m}} r_k \left(V_{(k)}^{-1/\alpha} \wedge \frac{E_k R_k^{1/\alpha}}{\beta}\right) f_n(t, U_k; H, \alpha)\right\}_{t\in[0,T]}, \quad (6.1)$$

where $Z_{\kappa,m}$ is a Poisson random variable with rate parameter $(T + \kappa)m$, $\{V_{(k)}\}_{k=1,...,Z_{\kappa,m}}$ are the ascending order statistics of $Z_{\kappa,m}$ many iid uniform random variables on $(0, m/c_\alpha)$, $\{U_k\}_{k\in\mathbb{N}}$ is a sequence of iid uniform random variables on $(-\kappa, T)$, $\{r_k\}_{k\in\mathbb{N}}$ is a sequence of iid Rademacher

random variables (taking values ± 1 with equal probability), $\{E_k\}_{k \in \mathbb{N}}$ is a sequence of iid exponential random variables with unit rate parameter, and $\{R_k\}_{k \in \mathbb{N}}$ is a sequence of iid uniform random variables on $(0,1)$.

Each term in the summation (6.1) has an intuitive explanation: the minimum term inside the brackets corresponds to the length of the kth jump for the driving tempered stable motion; the Rademacher random variable independently determines whether this jump is in the positive or negative direction (the equal probability of ± 1 ensures centrality), while the appearance of the uniform random variable in the higher order moving average kernel independently determines a random time for this kth jump to occur.

Due to this approximation in finite dimensional law, the fractional tempered stable motion is straightforward to (approximately) simulate in a manner similar to [32]. Namely, the process on the right hand side of (6.1) can be easily simulated on any discrete time grid $\{0, t_1, t_2, \ldots, t_{k-2}, t_{k-1}, T\}$ (or indeed at just one timepoint). This method of sampling boasts several advantages over Euler-Maruyama discretization schemes since they may be sampled at individual timepoints rather than progressively in increments. This means that supersampling (resampling on a finer timegrid once a simulation has already been performed) may be done without discarding any information, and that individual timepoints may be sampled accurately without thought to discretization error or the necessity to generate any previous timepoints. The histograms in Fig. 2 empirically demonstrate the convergences (5.1) and (5.2) by comparison to the known limits in distribution as $h \to 0$ and $h \to \infty$, respectively. In the Appendixes we include a note on exactly how to perform simulations on different timescales using the finite series approximation, since this cannot be done simply replacing $t \to ht$ on the right hand side of (6.1) as one might intuitively expect, due to truncation error.

VII. SIMULATION STUDY

We now turn our attention to the task of estimating parameters given data on sample trajectories, which we demonstrate by means of a Monte Carlo investigation. Arguably the most important tools for parameter inference in this context are the second order properties, particularly autocorrelation since it allows for estimation in principle off a single trajectory, and contains no influence from the parameters α and β related to the driving noise $\{L_t^{\alpha,\beta}\}_{t \in \mathbb{R}}$. This makes estimation more robust as data depends on fewer parameters, specifically only those associated with the kernel. Estimating parameters from the autocorrelation of the gray noise (4.5) to estimate the parameter G is only possible if the order n is known (so that it is known how many times differencing is needed to be performed to yield stationary gray noise). However, the relationship $G \in (n-1, n) \Rightarrow n = \lceil G \rceil$ shows that the estimated value of G enforces an estimate of n, demonstrating the inseparability of the G and n parameters and thus that the two parameters must be estimated in unison using successive differencing and autocorrelation (4.5).

In particular, for a range of parameter sets, we simulated sample trajectories of the n-ftsm were generated by means of the simulation scheme (6.1) on a linearly spaced time

TABLE I. Table of results estimating G for various parameter sets. In each case, we set $H = n - 1/2$ and performed 100 simulations for each parameter combination. Reported values in each cell are $[\text{mean}(\widehat{G}), \text{MSE}(\widehat{G})]$ for that parameter combination.

(α, β)	n = 2	3	4
(1.1,0.1)	$G = 1.09$ $(1.09, 5.3 \times 10^{-2})$	$G = 2.09$ $(2.14, 2.5 \times 10^{-2})$	$G = 3.09$ $(3.49, 0.17)$
(1.6,0.1)	$G = 1.375$ $(1.37, 1.6 \times 10^{-2})$	$G = 2.375$ $(2.40, 2.5 \times 10^{-2})$	$G = 3.375$ $(3.51, 2.8 \times 10^{-2})$
(1.1,1)	$G = 1.09$ $(1.09, 2.2 \times 10^{-2})$	$G = 2.09$ $(2.13, 2.8 \times 10^{-2})$	$G = 3.09$ $(3.49, 0.18)$
(1.6,1)	$G = 1.375$ $(1.37, 7 \times 10^{-3})$	$G = 2.375$ $(2.41, 1.9 \times 10^{-2})$	$G = 3.375$ $(3.52, 0.04)$
(1.1,10)	$G = 1.09$ $(1.09, 1.2 \times 10^{-2})$	$G = 2.09$ $(2.17, 5.5 \times 10^{-2})$	$G = 3.09$ $(3.49, 1.08)$
(1.6,10)	$G = 1.375$ $(1.37, 9 \times 10^{-2})$	$G = 2.375$ $(2.40, 0.17)$	$G = 3.375$ $(3.53, 0.05)$

grid of the form $\{jh\}_{j=0,1,\ldots,10^3}$ with $h := 0.1$. The order n was first estimated by determining the order of differencing required to render the observed time series weakly stationary. We used an augmented Dicky-Fuller test using MATLAB's inbuilt "adftest" function to test stationarity, differenced, and repeated as necessary, eventually recording the number of successive differencings required before the null hypothesis of stationarity was not rejected. Then, the sample autocorrelation function of the resulting series, interpreted as a sample of the fractional gray noise $\Delta_h^n L_{H,\alpha,\beta}^n(t)$, was calculated for lags at indices $0, 1, \ldots, 100$, where the sample autocovariance at lag index j for a time series of N total observations was defined as

$$a_N(j) := \frac{1}{n} \sum_{t=1}^{n-j} (Y_{t+j} - \overline{Y}_N)(Y_t - \overline{Y}_N),$$
$$j = 1, 2, \ldots, n-1. \tag{7.1}$$

and the corresponding autocorrelation given by the self-normalized value $\gamma(j) := a_N(j)/a_N(0)$. These sample autocorrelation values were then compared to the theoretical values implied by the autocorrelation (4.5) with a value of G fitted such that the sum of squared differences between theoretical and observed autocorrelations was minimized. This minimization was performed using the inbuilt MATLAB "fminunc" function with an initial guess for G of $\widehat{n} - 0.5$, where $\widehat{n}$ was the estimated value of the order n. The results are shown in Table I and a confusion matrix for estimating n is shown in Table II.

TABLE II. Confusion matrix for estimating n. In total, 100 simulations were performed on each of the six parameter sets from Table I, so the sum of each row of the confusion matrix is 600.

	$\widehat{n} = 2$	$\widehat{n} = 3$	$\widehat{n} = 4$	$\widehat{n} = 5$
$n = 2$	597	3	0	0
$n = 3$	0	598	2	0
$n = 4$	0	0	594	6

An obvious potential drawback of this pipeline for estimating n and G is that if the order n is incorrectly estimated, then the resulting $\widehat{n}$-times differenced time series cannot be interpreted as stationary gray noise and thus autocorrelation (4.5) does not hold. However, the "adftest" method of detecting stationarity lead to very accurate results as demonstrated in the confusion matrix, so this problem need not be encountered often in practice. In general the good agreement between estimated and true parameters demonstrates that parameter fitting can be performed reasonably well without too much overhead in terms of data collection.

We do not include estimation for the parameters α and β from the driving noise since this is, although feasible in theory from the $\widehat{n}$-times differenced sample trajectory, not straightforward in practice and worthy of its own investigation beyond the scope of this paper. We discuss potential approaches and obstacles to this estimation task in the Appendixes.

VIII. CONCLUSION AND DISCUSSION

We have introduced the higher order fractional tempered stable motion motivated by generalizing aspects of higher order fractional stable motion and higher order fractional Brownian motion [15,32]. The resulting stochastic process has the ability to capture time series data that has correlations that are too persistent to aptly be described by first order fractional processes, as in the n-fBm and the n-fsm. However, we generalized to tempered stable motion as the background noise because of the practical advantage of modeling transient distributions and admitting a well-defined covariance structure. Particularly, being stablelike on short timeframes and Gaussian in the long run, the n-ftsm has the capacity to model time series data whose background noise is in some sense "in between" the high activity of the stable motion, and the more passive Gaussian process. The rate of convergence to the eventual Gaussian process is determined by the generalized Hurst parameter which is a function of the level of persistence of correlations in sample trajectories and the stability index of the jump process in the underlying noise process. Therefore, the specifics of crossover dynamics from stable to Gaussian are controlled by physical parameters and may therefore by designed to suit experimental data in a non–*ad hoc* manner. Moreover, the tempered stable motion as driving noise possesses many technical advantages over the n-fsm. In particular, we have shown that the n-ftsm possess a finite second moment which has a specific form such that parameters may be chosen to model sub-, regular, super-, or hyperdiffusion. Finally, since the tempered stable motion is a Lévy process, an infinite shot noise representation of the n-ftsm may be designed as a basis for simulations. We introduced this simulation method for the n-ftsm so that it may form a basis for future Monte Carlo studies, and implemented it ourselves in order to demonstrate typical trajectories and the transient distributional behavior empirically. Finally, we presented a Monte Carlo study of parameter inference based on simulated data and showed that successive differencing and testing for stationarity to estimate the order n and least squares fitting between sample autocorrelation of gray noise and the autocorrelation (4.5) for G were good estimation techniques in this context.

The n-ftsm has extremely persistent correlations, to the extent that not only do correlations not decay quickly as the increments being correlated depart, but for appropriately large n, the correlation between departing increments in fact increase in time. This comes about due to the underlying sample path integration mechanism that yields higher order motions from lower order ones. This somewhat physically counterintuitive correlation increase with time suggests that the n-ftsm as a model for a position process would most likely find its best application in the $n = 2$ and $n = 3$ cases where the underlying velocity or acceleration (respectively) process driving the particle is a first order fractional tempered stable motion. For example, if the fluctuations of a stochastic (in space) force inducing an acceleration on a test particle, such as a magnet [47–49], electric field [50], or intracellular motor [51], for example, were to follow the first order fractional tempered stable motion, then the velocity and position processes of test particles would follow a 2-ftsm and 3-ftsm, respectively. In such cases, the successive integration not only smooths out the physical motion of the test particle, but forces particles' directions to point decisively in one direction after a short period of time [this is illustrated in (b) and (d) in Fig. 1]. We note though that, although these persistent path properties occur, the mean squared displacement conveniently remains finite for all time and obeys a power-law scaling with respect to time in agreement with canonical anomalous diffusion models.

In regards to future directions of research, we remark that the simulation study we presented for parameter inference, while aptly demonstrating the suitability of classical parameter estimation procedures, is by no means a comprehensive study of the subject. In particular, theoretical convergence results for the parameters that were estimated remain unknown. Further, a thorough investigation into the performance of various estimation procedures for fitting the parameters of the stationary gray noise time series that emerges after successive differencing is worthy of its own separate investigation. The competition of performance between various methods of parameter fitting on the fractional gray noise will be especially pertinent when experimental data, rather than computer simulated data, is to be fitted to the higher order fractional tempered stable motion.

APPENDIX A: DERIVATION OF THE COVARIANCE AND MEMORY

In this section we derive the covariance of the n-ftsm. Recall that $G = H - 1/\alpha + 1/2$ and that $\{B_G^n(t)\}_{t \geqslant 0}$ is the n-fBm [15]. Define $R_{H,\alpha,\beta}^n(s, t) := \mathrm{Cov}(L_{H,\alpha,\beta}^n(s), L_{H,\alpha,\beta}^n(t))$. The covariance structure (4.1) of the n-ftsm can be calculated recursively using the relation

$$R_{H,\alpha,\beta}^n(s, t) = \int_0^t \int_0^s R_{H-1,\alpha,\beta}^{n-1}(u, v) \, du \, dv, \tag{A1}$$

which follows from the relation (3.1). The integrals in (A1) start at the origin (rather than at negative infinity) because, unlike the tempered stable integrator which takes values at negative times, this integral is of the covariance function of n-ftsm which only has values at positive times.

The base case, $n = 1$, emerges from the Wiener-Itô isometry. In particular, for $0 \leqslant s \leqslant t$,

$$
\begin{aligned}
R^1_{H,\alpha,\beta}(s,t) &= \mathbb{E}\big[L^1_{H,\alpha,\beta}(s)L^1_{H,\alpha,\beta}(t)\big] \\
&= \gamma^2_{\alpha,\beta} \int_{\mathbb{R}} f_1(s,u;H,\alpha)f_1(t,u;H,\alpha)du \\
&= \gamma^2_{\alpha,\beta} \int_{\mathbb{R}} f_1(s,u;G,2)f_1(t,u;G,2)du \\
&= \gamma^2_{\alpha,\beta} \mathrm{Var}(B^1_G(1))\big(t^{2G} + s^{2G} - (t-s)^{2G}\big),
\end{aligned}
\tag{A2}
$$

where the second line is the Wiener-Itô isometry and the final line is the covariance structure for the fractional Brownian motion, since f_1 denotes the usual first order moving average kernel [12]. In particular, $\mathrm{Var}(B^1_G(1)) = 1/[\Gamma(2G+1)\sin(\pi G)]$, the variance of the unit time marginal of the first order fBm. Then, assuming the covariance structure (4.1) holds for the $(n-1)$-ftsm with Hurst parameter $H-1$, we get

$$
\begin{aligned}
R^n_{H,\alpha,\beta}(s,t) &= \gamma^2_{\alpha,\beta}C^{n-1}_{G-1} \int_0^t \int_0^s \left[(u-v)^{2G-2} - \sum_{j=0}^{n-2}(-1)^j \binom{2G-2}{j}\left(\left(\frac{u}{v}\right)^j v^{2G-2} + \left(\frac{v}{u}\right)^j u^{2G-2}\right)\right] du\,dv \\
&= \frac{1}{2G(2G-1)}\gamma^2_{\alpha,\beta}C^{n-1}_{G-1}\left[(t-s)^{2G} - s^{2G} - t^{2G} - \sum_{k=1}^{n-1}(-1)^k \binom{2G}{k}\left(\left(\frac{t}{s}\right)^k s^{2G} + \left(\frac{s}{t}\right)^k t^{2G}\right)\right] \\
&= \frac{\gamma^2_{\alpha,\beta}C^{n-1}_{G-1}}{2G(2G-1)}\left[(t-s)^{2G} - \sum_{j=0}^{n-1}(-1)^j \binom{2G}{j}\left(\left(\frac{t}{s}\right)^j s^{2G} + \left(\frac{s}{t}\right)^j t^{2G}\right)\right],
\end{aligned}
\tag{A3}
$$

which, since the s^{2G} and t^{2G} terms in the second last line get absorbed into the sum with a change of limits in the last line, gives the desired result by mathematical induction, provided that the constant C^n_G is the solution to the recurrence relation

$$
C^1_G = \frac{1}{\Gamma(2G+1)\sin(\pi G)}, \quad C^n_G = \frac{C^{n-1}_{G-1}}{2G(2G-1)},
\tag{A4}
$$

which turns out to be $C^n_G = [\Gamma(2G+1)|\sin(\pi G)|]^{-1}$ as claimed. Having the above result, we can write the covariance term in the definition of long memory in the following way:

$$
\mathrm{Cov}\big(\Delta_h L^n_{H,\alpha,\beta}(0), \Delta_h L^n_{H,\alpha,\beta}(t)\big)
$$

$$
= \gamma^2_{\alpha,\beta}C^n_G\left[t^{2G} - (t-h)^{2G} - \sum_{j=1}^{n-1}(-1)^j \binom{2G}{j}\big(t^j h^{2G-j}(1-(1+h/t)^j) + t^{2G-j}h^j(1-(1+h/t)^{2G-j})\big)\right].
\tag{A5}
$$

Recalling the Taylor series for $(t-h)^{2G} = t^{2G}(1-h/t)^{2G}$ in h around zero,

$$
t^{2G}(1 \pm h/t)^{2G} = \sum_{j=0}^{n-1}(\pm 1)^j \binom{2G}{j}h^j t^{2G-j} + O(h^n),
\tag{A6}
$$

and carefully expanding the sums in the covariance expression (A5) one term at a time (Taylor expanding individual summands themselves where necessary), we obtain

$$
\mathrm{Cov}\big(L^n_{H,\alpha,\beta}(h), \Delta_h L^n_{H,\alpha,\beta}(t)\big)
$$

$$
\begin{aligned}
&= \gamma^2_{\alpha,\beta}C^n_G\Bigg[2(G-1)h^2 t^{2(G-1)} + \sum_{j=3}^{n-1}(-1)^j \binom{2G}{j}\big(t^j h^{2G-j}(1-(1+h/t)^j) + t^{2G-j}h^j(1-(1+h/t)^{2G-j})\big) \\
&\quad + t^{2G-2}\sum_{j=1}^{n-1}\binom{2G-2}{j}h^j t^{-j} + O(h^n)\Bigg] \sim 2(G-1)\gamma^2_{\alpha,\beta}C^n_G h^2 t^{2(G-1)},
\end{aligned}
\tag{A7}
$$

hence the leading order of $t^{2(G-1)}$ as $t \to \infty$ reported in the asymptotic expression (4.3). The lower limit on the first summation in (A7) is $j = 3$ because the $j = 1$ term cancels and the $j = 2$ term gives the $2(G-1)h^2 t^{2(G-1)}$ term which was left out the front of the summation for emphasis since this is the dominating term in the large t regime.

APPENDIX B: DETAILS ABOUT THE DRIVING NOISE: TEMPERED STABLE MOTION

The marginal distribution of the tempered stable motion we used to define the n-ftsm is symmetric due to the symmetry of its characteristic function. This motion can be defined more generally to allow for asymmetry in jump distributions but we do not consider this in the present paper, since this generalization would not contribute much qualitatively relative to the technical complication it would bring. For completeness' sake we note that in Rosinski's multidimensional definition [28], the most general definition of a tempered stable process, a Lévy process without Gaussian component is called tempered stable if its Lévy measure is of the form

$$\nu(B) = \int_{\mathbb{R}^d \setminus \{0\}} \int_0^\infty \mathbb{1}_B(sx) s^{-\alpha-1} e^{-s} ds \, \rho(dx), \qquad \text{(B1)}$$

for a set $B \in \mathscr{B}(\mathbb{R}^d \setminus \{0\})$, the Borel σ field on $\mathbb{R}^d \setminus \{0\}$. The measure ρ is called the inner measure and must satisfy the condition $\int_{\mathbb{R}^d \setminus \{0\}} \|x\|^\alpha \rho(dx) < \infty$. An elementary calculation reveals that our tempered stable motion $\{L_t^{\alpha,\beta}\}_{t \geq 0}$ from Sec. II is generated by an inner measure of the form $\rho(dx) = \delta_{\{-1/\beta\}}(dx) + \delta_{\{1/\beta\}}(dx)$ (up to a constant), which satisfies the required integrability condition. In particular, this means that a similar argument to the proof of [38, Proposition 2.5] demonstrates that the marginals of the n-ftsm are tempered stable with inner measure $\eta_t := M \circ J_t$, where $M(dx, ds) = (\delta_{\{-1/\beta\}}(dx) + \delta_{\{1/\beta\}}(dx))ds$ and $J_t(B) = \{(x, s) \in \mathbb{R} \setminus \{0\} \times [0, t] : x f_n(t, s; H, \alpha) \in B\}$ for $B \in \mathscr{B}(\mathbb{R}^d \setminus \{0\})$. Since $\int_{\mathbb{R} \setminus \{0\}} x^2 (\delta_{\{1/\beta\}}(dx) + \delta_{\{-1/\beta\}}(dx)) < \infty$, this implies that the pth moment of the n-ftsm is finite for all $p \geq 0$, provided the kernel is in $L^p(\mathbb{R})$, for which conditions are found in Appendix C.

The characteristic function (2.2) is that of the unit time marginal of the tempered stable motion $L_1^{\alpha,\beta}$. This can be generalized to all $t \in \mathbb{R}$ since the tempered stable motion is a Lévy process, and hence the characteristic exponent at any time $t \in \mathbb{R}$ may be obtained by multiplying the characteristic exponent (2.2) by $|t|$. Strictly speaking, for the time index to run over all $t \in \mathbb{R}$ it is necessary to run two independent tempered stable motions forward in time, reflect one such that it runs over $(-\infty, 0)$, and rejoin the processes at the origin (making the appropriate modifications to the backwards running tempered stable motion such that the total process retains the càdlàg property) [40]. The purpose for incorporating the negative values of t into the definition of the tempered stable motion is to allow the integration kernel (2.1) to be integrated over its entire support, not merely the positive part. The integral (2.2) always converges at infinity regardless of tempering and converges around the origin thanks to the compensation term "$-iyz$."

The second moment of the tempered stable distribution may be calculated using the characteristic function (2.2). In particular, we have

$$\gamma_{\alpha,\beta}^2 = -\lim_{y \to 0} \frac{d^2}{dy^2} \phi_{\alpha,\beta}(y) = \int_{\mathbb{R} \setminus \{0\}} z^2 \nu(dz) = \frac{\alpha(1-\alpha)\beta^{\alpha-2}}{\cos(\pi\alpha/2)}. \qquad \text{(B2)}$$

APPENDIX C: DETAILS ABOUT THE INTEGRATION KERNEL

The choice to define the kernel (II.1) for the n-ftsm as a modification of the usual moving average instead of, for example, the Volterra kernel of [38] was made because it is more intuitive how this kernel may be adapted to describe "higher order" correlations. Namely, the higher order moving average kernel considers the "tail" of the Taylor series for the moving average function $(t - s)_+^{H-1/\alpha}$ around s, by subtracting off the first n terms of the expansion [15]. The trade-off for this intuitive definition is the fact that the domain of integration must be taken to be the semi-infinite interval $(-\infty, t]$ instead of the compact domain $[0, t]$, as in the case of the Volterra kernel of [38]. This means that the infinite series representation of the n-ftsm, which we introduce in Sec. VI as a simulation method, must be truncated in practice, leading to truncation error in sample path simulation.

Due to the asymptotics of the kernel [32], it can be shown that $f_n(t, \cdot; 1/\alpha) \in L^p(\mathbb{R})$ for $p \geq 2$ if and only if $H \in (1/\alpha - 1/p + n - 1, 1/\alpha - 1/p + n)$.

We note that, with reference to the kernel (2.1), it is impossible to distinguish the parameters H and α as they always appear together in the form of the parameter $H - 1/\alpha$. In fact, the kernel may be written in infinitely many different ways as $f_n(t, s; H, \alpha) = f_n(t, s; H - 1/\alpha + 1/\eta, \eta)$, where η may take any value (in particular $(0,2]$ was relevant for our purposes). Nevertheless, we chose to write the parameters H and α separately when denoting the kernel $f_n(\cdot, \cdot; H, \alpha)$ because they came from two different sources: α is a parameter in the background noise $\{L_t^{\alpha,\beta}\}_{t \geq 0}$ while H is a property introduced exclusively in the kernel concerning the persistence of correlations of sample paths. Moreover, as we showed in Sec. III, the pathwise differentiation and integration of the n-ftsm affects the parameters n and H concerned with the order of correlations, while leaving the parameter α unchanged. For the well definedness of the n-ftsm, it is necessary that $G \in (n - 1, n)$ so that the long-run limiting n-fBm is well defined), which brings about the restriction $H - 1/\alpha \in (n - 3/2, n - 1/2)$ as stipulated in Definition II.1.

APPENDIX D: NOTE ON SHORT AND LONG RUN CONVERGENCES

As mentioned in Sec. V, the convergences (5.1) and (5.2) may be demonstrated by means of convergence in characteristic function of linear combinations of the n-ftsm at various times (convergence of finite dimensional distributions). However, an intuitive demonstration of these convergences may be given by demonstrating convergence in distribution directly.

Recalling that from [28] the rescaled process $\{h^{-1/\alpha} L_{ht}^{\alpha,\beta}\}_{t \geq 0}$ tends to $\{L_t^\alpha\}_{t \geq 0}$, a symmetric stable Lévy

motion with Lévy measure $c_\alpha/|z|^{1+\alpha} dz$, in finite dimensional distribution as $h \to 0$, while $\{h^{-1/2} L_{ht}^{\alpha,\beta}\}_{t \geqslant 0}$ tends to $\{cW_t\}_{t \geqslant 0}$ in the same sense, for the appropriate constant $c \in \mathbb{R}$, by the central limit theorem and noting that $f_n(ht, hs; H, \alpha) = h^{H-1/\alpha} f_n(t, s; H, \alpha)$, it is straightforward to make the direct observation

$$
\begin{aligned}
h^{-H} L_{H,\alpha,\beta}^n(ht) &= h^{-H} \int_{-\infty}^{ht} \int_{\mathbb{R}} f_n(ht, s; H, \alpha) dL_s^{\alpha,\beta} \\
&= h^{-H} \int_{-\infty}^{t} \int_{\mathbb{R}} f_n(ht, hs; H, \alpha) dL_{hs}^{\alpha,\beta} \\
&= \int_{-\infty}^{t} \int_{\mathbb{R}} f_n(t, s; H, \alpha) \left(h^{-1/\alpha} dL_{hs}^{\alpha,\beta} \right) \\
&\to \int_{-\infty}^{t} \int_{\mathbb{R}} f_n(t, s; H, \alpha) dL_s^{\alpha}, \quad \text{(D1)}
\end{aligned}
$$

as $h \to 0$, generating the n-fsm [32]. Similarly,

$$
\begin{aligned}
h^{-G} L_{H,\alpha,\beta}^n(ht) &= h^{-G} \int_{-\infty}^{ht} f_n(ht, s; H, \alpha) dL_s^{\alpha,\beta} \\
&= \int_{-\infty}^{t} f_n(t, s; H, \alpha) d \left(h^{-1/2} L_{hs}^{\alpha,\beta} \right) \\
&\to \int_{-\infty}^{t} f_n(t, s; H, \alpha) \gamma_{\alpha,\beta} dW_s \\
&= \gamma_{\alpha,\beta} \int_{-\infty}^{t} f_n(t, s; G, 2) dW_s = \gamma_{\alpha,\beta} B_G^n(t),
\end{aligned}
$$
(D2)

as $h \to \infty$, where $\{W_t\}_{t \geqslant 0}$ is the standard Brownian motion in $\mathbb{R}$ and $\{B_G^n(t)\}_{t \geqslant 0}$ is the n-fBm [15]. The finite upper limit on these integrals is justified by the fact that the kernel is zero for $s > t$. This illustrates the short and long run convergences (5.1) and (5.2) of the n-ftsm.

APPENDIX E: NOTE ON THE SIMULATION METHOD

The simulation method (6.1) is based on the representation of the n-ftsm in terms of compensated Poisson random measures. Namely, if we introduce the Poisson random measure $\mu(dz, ds)$ whose compensator is $\nu(dz)ds$, we can write the underlying tempered stable motion in the Lévy-Itô form $dL_s^{\alpha,\beta} = \int_{\mathbb{R} \setminus \{0\}} z(\mu - \nu)(dz, ds)$. Now, we note that the Poisson random measure μ is infinite in the sense that the nonintegrability of the Lévy measure ν around the origin ensures an infinite number of "small" jumps close to the origin. Therefore, in simulation, truncation must be performed not just with respect to the infinite time horizon of the driving noise, but also with respect to its infinite intensity of jumps. Concretely, the simulation scheme (6.1) on a compact time interval $[0, T]$ is an exact representation of the approximating process

$$
\begin{aligned}
&\left\{ L_{H,\alpha,\beta}^n(t; \kappa, m) \right\}_{t \in [0,T]} \\
&:= \left\{ \int_{-\kappa}^{t} \int_{|z| > \eta(m)} f_n(t, s; H, \alpha) z(\mu - \nu)(dz, ds) \right\}_{t \in [0,T]},
\end{aligned}
$$
(E1)

where $\eta(m) := (m/c_a)^{-1/\alpha}$ reflects the truncation level of the underlying Lévy measure around the origin and $-\kappa$ is the truncation time of the underlying tempered stable noise towards negative infinity; see [32,52] for details and specifics on error analysis. Then, in investigating the short and long run behaviors of this approximating process, we are interested in (up to a constant) rescaling the time of the approximating process. To do this accurately, however, we note that this requires also rescaling the truncation time κ to $h\kappa$, since this gives

$$
\begin{aligned}
&\left\{ L_{H,\alpha,\beta}^n(ht; h\kappa, m) \right\}_{t \in [0,T]} \\
&= \left\{ \int_{-\kappa}^{t} \int_{|z| > \eta(m)} f_n(t, s; H, \alpha) z(\mu - \nu)(dz, hds) \right\}_{t \in [0,T]},
\end{aligned}
$$
(E2)

as desired. Applying the naive transformation $t \to ht$ alone will prevent the desired convergence from emerging since this would change the truncated window of time over which the driving noise is allowed to run (we would have $-\kappa/h$ as the bottom limit on the outer integral). It is therefore necessary to examine the asymptotic behavior of $\{h^{-K} L_{H,\alpha,\beta}^n(ht; h\kappa, m)\}_{t \in [0,T]}$ (for the appropriate constant $K = H$ or G) to observe the convergences (5.1) and (5.2) empirically.

APPENDIX F: NOTES ON SIMULATION STUDY

In the simulation study in Sec. VII, the method of curve fitting was chosen over, for example, finding G such that the sample and theoretical autocorrelation values at lag 1 aligned exactly, because it gave more reliable results, which was unsurprising since this method takes more data points into consideration and thus averages out statistical noise.

Once the fractional gray noise has been obtained, it may be interpreted as a time series with a tempered stable distribution and therefore the α and β parameters may in principle be estimated using standard statistical estimators like the method of moments or maximum likelihood estimation [53–55]. However, within the context of fractional gray noises, the best way to do this is not decided. On the one hand, for method of moments, the symmetry of the driving noise in our case, rendering all odd moments (especially the first and third) zero and thus not useful for parameter inference and the fact that two parameters are to be estimated forces the second and fourth moment to be considered. This could be considered due to the closed form availability of these moments as $\mathbb{E}[(L_1^{\alpha,\beta})^2] = \beta^{\alpha-2} \alpha(1 - \alpha)/\cos(\pi\alpha/2)$ and

$$
\mathbb{E}\left[\left(L_1^{\alpha,\beta} \right)^4 \right] = 3(\gamma_{\alpha,\beta}^2)^2 + \frac{\alpha(1-\alpha)(2-\alpha)(3-\alpha)\beta^{\alpha-4}}{\cos(\pi\alpha/2)}.
$$

However, the fourth moment is a very noisy measurement in this context given the presence of regular statistical fluctuations coexisting with discretization error from differencing and truncation error in the underlying driving noise simulation. On the other hand, the maximum likelihood estimator is not available in closed form due to the non-Gaussianity we have introduced here. It could be approached numerically with appropriate density estimation but again this is not straightforward and an appropriately rigorous treatment of this is beyond the scope of the current paper.

[1] M. Fettach, A. Hassini, A. Hamdoun, and L. Driouch, Magnetic study of amorphous $Fe_{91-x}Y_xZr_9$ alloys, Phys. B: Condens. Matter **325**, 203 (2003).

[2] J. Čermák and I. Stloukal, Diffusion and structural changes in $Fe_{91-y}Mo_8Cu_1B_y$ alloys, J. Phys.: Condens. Matter **19**, 156219 (2007).

[3] G. Q. Zhu, J. Boeuf, and B. Chaudhury, Ionization-diffusion plasma front propagation in a microwave field, Plasma Sources Sci. Technol. **20**, 035007 (2011).

[4] Y. Fukai, Hydrogen diffusion in metals, Defect Diffus. Forum **95–98**, 297 (1993).

[5] D. S. Banks and C. Fradin, Anomalous diffusion of proteins due to molecular crowding, Biophys. J. **89**, 2960 (2005).

[6] M. Weiss, M. Elsner, F. Kartberg, and T. Nilsson, Anomalous subdiffusion is a measure for cytoplasmic crowding in living cells, Biophys. J. **87**, 3518 (2004).

[7] G. Guigas and M. Weiss, Sampling the cell with anomalous diffusion–the discovery of slowness, Biophys. J. **94**, 90 (2008).

[8] A. Shalchi, Time-dependent transport and subdiffusion of cosmic rays, J. Geophys. Res. **110**, A09103 (2005).

[9] A. A. Lagutin and V. V. Uchaikin, Anomalous diffusion equation: Application to cosmic ray transport, Nucl. Instrum. Methods Phys. Res. B **201**, 212 (2003).

[10] A. Stanislavsky and K. Weron, Transport of magnetic bright points on the Sun. Analysis of subdiffusion scenarios, Astrophys. Space Sci. **323**, 351 (2009).

[11] J. Kóta and J. R. Jokipii, Velocity correlation and the spatial diffusion coefficients of cosmic rays: Compound diffusion, Astrophys. J. **531**, 1067 (2000).

[12] B. B. Mandelbrot and J. W. Van Ness, Fractional Brownian motions, fractional noises and applications, SIAM Rev. **10**, 422 (1968).

[13] J. Beran, *Statistics for Long-Memory Processes* (Routledge, London, 2017).

[14] T. Loussot, R. Harba, G. Jacquet, C. L. Benhamou, E. Lespessailles, and A. Julien, An oriented fractal analysis for the characterization of texture. Application to bone radiographs, in *European Signal Processing Conference, 1996*, 8th ed. (IEEE, New York, 1996), pp. 1–4.

[15] E. Perrin, R. Harba, C. Berzin-Joseph, I. Iribarren, and A. Bonami, nth-order fractional Brownian motion and fractional Gaussian noises, IEEE Trans. Signal Process. **49**, 1049 (2001).

[16] J. Klafter and I. M. Sokolov, Anomalous diffusion spreads its wings, Phys. World **18**, 29 (2005).

[17] R. N. Mantegna and H. E. Stanley, Econophysics: Scaling and its breakdown in finance, J. Stat. Phys. **89**, 469 (1997).

[18] M. C. Mariani and Y. Liu, Normalized truncated Lévy walks applied to the study of financial indices, Physica A **377**, 590 (2007).

[19] P. Carr and L. Wu, The finite moment log stable process and option pricing, J. Finance **58**, 753 (2003).

[20] M. F. Shlesinger, B. J. West, and J. Klafter, Lévy Dynamics of Enhanced Diffusion: Application to Turbulence, Phys. Rev. Lett. **58**, 1100 (1987).

[21] T. H. Solomon, E. R. Weeks, and H. L. Swinney, Observation of Anomalous Diffusion and Lévy Flights in a Two-Dimensional Rotating Flow, Phys. Rev. Lett. **71**, 3975 (1993).

[22] X. Yang and S. Deb, Cuckoo search via Lévy flights, in *World Congress on Nature & Biologically Inspired Computing* (IEEE, New York, 2009), pp. 210–214.

[23] A. M. Reynolds, A. D. Smith, R. Menzel, U. Greggers, D. R. Reynolds, and J. R. Riley, Displaced honey bees perform optimal scale-free search flights, Ecology **88**, 1955 (2007).

[24] G. Boccignone and M. Ferraro, Modelling gaze shift as a constrained random walk, Physica A **331**, 207 (2004).

[25] F. Bartumeus, Lévy processes in animal movement: An evolutionary hypothesis, Fractals **15**, 151 (2007).

[26] B. Baeumer and M. Meerschaert, Tempered stable Lévy motion and transient super-diffusion, J. Comput. Appl. Math. **233**, 2438 (2010).

[27] J. Janczura and A. Wylomanska, Anomalous diffusion models: Different types of subordinator distribution, Acta Phys. Pol. B **43**, 1001 (2012).

[28] J. Rosiński, Tempering stable processes, Stochast. Process. Appl. **117**, 677 (2007).

[29] S. Carnaffan and R. Kawai, Cusping, transport and variance of solutions to generalized Fokker-Planck equations, J. Phys. A: Math. Theor. **50**, 245001 (2017).

[30] S. Carnaffan and R. Kawai, Solving multidimensional fractional Fokker-Planck equations via unbiased density formulas for anomalous diffusion processes, SIAM J. Sci. Comput. **39**, B886 (2017).

[31] F. Sabzikar, M. Meerschaert, and J. Chen, Tempered fractional calculus, J. Comput. Phys. **293**, 14 (2015).

[32] R. Kawai, Higher order fractional stable motion: Hyperdiffusion with heavy tails, J. Stat. Phys. **165**, 126 (2016).

[33] A. Stanislavsky and A. Weron, Transient anomalous diffusion with Prabhakar-type memory, J. Chem. Phys. **149**, 044107 (2018).

[34] I. Bronstein, Y. Israel, E. Kepten, S. Mai, Y. Shav-Tal, E. Barkai, and Y. Garini, Transient Anomalous Diffusion of Telomeres in the Nucleus of Mammalian Cells, Phys. Rev. Lett. **103**, 018102 (2009).

[35] M. Latini and A. J. Bernoff, Transient anomalous diffusion in Poiseuille flow, J. Fluid Mech. **441**, 399 (2001).

[36] M. J. Saxton, A biological interpretation of transient anomalous subdiffusion. I. Qualitative model, Biophys. J. **92**, 1178 (2007).

[37] I. Koponen, Analytic approach to the problem of convergence of truncated Lévy flights towards the Gaussian stochastic process, Phys. Rev. E **52**, 1197 (1995).

[38] C. Houdré and R. Kawai, On fractional tempered stable motion, Stoch. Process. Applicat. **116**, 1161 (2006).

[39] M. Riedel, Representation of the characteristic function of a stochastic integral, J. Appl. Probab. **17**, 448 (1980).

[40] G. Samorodnitsky and M. S. Taqqu, *Stable Non-Gaussian Random Processes* (Chapman and Hall, London, 1994).

[41] R. T. Baillie, Long memory processes and fractional integration in econometrics, J. Econometrics **73**, 5 (1996).

[42] F. Comte and E. Renault, Long memory in continuous-time stochastic volatility models, Math. Finance **8**, 291 (1998).

[43] A. C. Harvey, Long memory in stochastic volatility, in *Forecasting Volatility in the Financial Markets*, 3rd ed. (Elsevier, Amsterdam, 2007), pp. 351–363.

[44] M. M. Meerschaert, F. Sabzikar, M. S. Phanikumar, and A. Zeleke, Tempered fractional time series model for turbulence in geophysical flows, J. Stat. Mech. (2014) P09023.

[45] V. Cvetkovic, The tempered one-sided stable density: a universal model for hydrological transport? Environ. Res. Lett. **6**, 034008 (2011).

[46] J. Imai and R. Kawai, Numerical inverse Lévy measure method for infinite shot noise series representation, J. Comput. Appl. Math. **253**, 264 (2013).

[47] A. R. Jacobson and R. W. Moses, Nonlocal dc electrical conductivity of a Lorentz plasma in a stochastic magnetic field, Phys. Rev. A **29**, 3335 (1984).

[48] A. B. Rechester, M. N. Rosenbluth, and R. B. White, Calculation of the Kolmogorov Entropy for Motion Along a Stochastic Magnetic Field, Phys. Rev. Lett. **42**, 1247 (1979).

[49] A. Mack, T. Kahniashvili, and A. Kosowsky, Microwave background signatures of a primordial stochastic magnetic field, Phys. Rev. D **65**, 123004 (2002).

[50] I. P. Sugar and E. Neumann, Stochastic model for electric field-induced membrane pores electroporation, Biophys. Chem. **19**, 211 (1984).

[51] P. C. Bressloff and J. M. Newby, Stochastic models of intracellular transport, Rev. Mod. Phys. **85**, 135 (2013).

[52] J. Imai and R. Kawai, On finite truncation of infinite shot noise series representation of tempered stable laws, Physica A **390**, 4411 (2011).

[53] J. Gajda and A. Wyłomańska, Geometric Brownian motion with tempered stable waiting times, J. Stat. Phys. **148**, 296 (2012).

[54] S. Orzeł and A. Wyłomańska, Calibration of the subdiffusive arithmetic Brownian motion with tempered stable waiting-times, J. Stat. Phys. **143**, 447 (2011).

[55] A. Wyłomańska, Arithmetic Brownian motion subordinated by tempered stable and inverse tempered stable processes, Physica A **391**, 5685 (2012).